HHS Public Access

Author manuscript

Sci Transl Med. Author manuscript; available in PMC 2015 March 17.

Published in final edited form as:

Sci Transl Med. 2014 September 3; 6(252): 252ra120. doi:10.1126/scitranslmed.3008791.

Breast-fed and bottle-fed infant rhesus macaques develop distinct gut microbiotas and immune systems

Amir Ardeshir[1,*], **Nicole R. Narayan**[1,2,*], **Gema Méndez-Lagares**[1,2,*], **Ding Lu**[1,2], **Marcus Rauch**[3], **Yong Huang**[4], **Koen K. A. Van Rompay**[1], **Susan V. Lynch**[3], and **Dennis J. Hartigan-O'Connor**[1,2,5,†]

[1]California National Primate Research Center, University of California, Davis, Davis, CA 95616, USA

[2]Department of Medical Microbiology and Immunology, University of California, Davis, Davis, CA 95616, USA

[3]Division of Gastroenterology, Department of Medicine, University of California, San Francisco, San Francisco, CA 94143, USA

[4]Department of Bioengineering and Therapeutic Sciences, School of Pharmacy, University of California, San Francisco, San Francisco, CA 94143, USA

[5]Division of Experimental Medicine, Department of Medicine, University of California, San Francisco, San Francisco, CA 94143, USA

Abstract

Diet has a strong influence on the intestinal microbiota in both humans and animal models. It is well established that microbial colonization is required for normal development of the immune system and that specific microbial constituents prompt the differentiation or expansion of certain immune cell subsets. Nonetheless, it has been unclear how profoundly diet might shape the primate immune system or how durable the influence might be. We show that breast-fed and bottle-fed infant rhesus macaques develop markedly different immune systems, which remain different 6 months after weaning when the animals begin receiving identical diets. In particular, breast-fed infants develop robust populations of memory T cells as well as T helper 17 (T_H17) cells within the memory pool, whereas bottle-fed infants do not. These findings may partly explain the variation in human susceptibility to conditions with an immune basis, as well as the variable protection against certain infectious diseases.

†Corresponding author. E-mail: dhartigan@ucdavis.edu.
*These authors contributed equally to this work.

Author contributions: A.A., D.J.H.-O., and S.V.L. designed the study. A.A. and M.R. performed PhyloChip assays. A.A., N.R.N., M.R., and D.J.H.-O. performed the statistical analysis. A.A., N.R.N., G.M.-L., and D.J.H.-O. wrote the manuscript. G.M.-L. performed the flow cytometry assay and analysis. Y.H. performed the kyn/trp assay. D.L. and K.K.A.V.R. collected the samples.

Competing interests: S.V.L. consults for Janssen Pharmaceuticals and Theravance Biopharma and is on the Scientific Advisory Board of Second Genome. The other authors declare no competing interests.

Supplementary Materials: www.sciencetranslationalmedicine.org/cgi/content/full/6/252/252ra120/DC1
Fig. S1. Associations of *Campylobacter* with arachidonic acid concentrations and T_H17 cells.
Fig. S2. No significant differences found in tryptophan catabolism between rearing groups.
Table S1. Significant differences in taxa between rearing groups.

Introduction

The human and nonhuman primate gut microbiotas are extraordinarily diverse, vary between individuals, and can fluctuate over time in response to diet and environmental factors (1–3). The microbiota influences metabolic processes in the host, immune system development, responses to infection, and even behavioral abnormalities (4–10). For example, regulatory T cell (T_{reg}) activity in mice is stimulated by the human commensal *Bacteroides fragilis* (11), by certain Clostridia bacterial species (12, 13), and by short-chain fatty acids produced by bacteria after digestion of fiber (14). Similarly, segmented filamentous bacteria have been found to induce T helper 17 (T_H17) cells (15). More recently, McCune and colleagues have proposed that tryptophan cat-abolites produced by the gut microbiota are important regulators of T_H17-T_{reg} balance in HIV infection (16, 17).

T_H17 cells are particularly important for host defense against mu-cosal pathogens such as HIV and *Salmonella*. HIV-positive individuals exhibit highly variable rates of disease progression, as measured by viral load and $CD4^+$ T cell loss (18). This variability is only partly explained by host genetics (19, 20). Disease progression in humans is associated with T_H17 cell loss; on the other hand, simian immunodeficiency virus (SIV) replication in the rhesus macaque is limited by the size of the preexisting T_H17 cell compartment, possibly because of maintenance or enhancement of the gut mucosal barrier (21, 22). The progress of *Salmonella* infection is also influenced by T_H17 cell numbers in the host, with greater dissemination of bacteria from gut tissue to lymph nodes under low T_H17 conditions (23).

The gut microbiotas of infants are dynamic and highly dependent on a number of factors, including delivery method and diet (for example, breast-feeding versus formula-feeding). Numerous studies have found differences in the gut microbiotas of humans and nonhuman primates as a result of differences in early diet (24–27). Moreover, these microbial differences are associated with differences in baseline concentrations of circulating cytokines as well as serum and urine metabolites, including increases in proinflammatory cytokines [interleukin-1β (IL-1β), IL-1 receptor antagonist, and tumor necrosis factor–α] and amino acid metabolites in bottle-fed (nursery-reared) animals (25). These differences may be linked to immunopathologic consequences, because bottle-fed/nursery-reared infant macaques were 7.5 times more likely than dam-reared infants to develop idiopathic chronic diarrhea later in life (28).

Despite this abundance of suggestive data, no published studies directly link different infant diets and gut microbiotas to altered microbiota-derived metabolites and durable changes in the developing immune system. Changes in the immune system could affect the host response to infections and diseases occurring beyond infancy. To test the possible effects of the gut microbiota on immune system development, we followed breast-fed and bottle-fed infant rhesus macaques (all housed indoors) between 5 and 12 months of age. We found that early differences in feeding regimens were associated with divergent development of the immune system over both the short term and long term, including durable changes in immune ontogeny persisting after identical diets had been imposed.

Results

Infant macaques develop varying T_H17 cell populations at disparate rates

We previously demonstrated that adult rhesus macaques have widely disparate fractions of T_H17 cells among circulating and gut-resident $CD4^+$ T cells (29). We next examined T_H17 cell representation across the macaque life span to determine how quickly infant macaques generate normal adult frequencies of T_H17 cells. We plotted data gathered through analysis of samples from 125 different uninfected macaques followed in various studies carried out at the California National Primate Research Center (CNPRC) (Fig. 1).

These data confirmed our previous report of disparate T_H17 cell representation in adult animals, with such cells ranging between 0.9 and 8.5% of circulating cells in animals over 18 months (547 days) old, without any apparent significant change beyond that age (Fig. 1A). More limited data on absolute counts of circulating T_H17 cells also suggested no significant change after 18 months (Fig. 1B). Quantitation of gut tissue–resident T_H17 cells was not attempted, but in previous studies, we have found that the percentage of circulating T_H17 cells correlated with the percentage of T_H17 cells found in colon tissue (29).

Most importantly, we found that newborn macaques harbor few T_H17 cells and that these cells develop progressively throughout the first 18 months of life (Fig. 1C). Surprisingly, the rate of development of T_H17 cells in infancy was markedly variable, with some individuals rapidly developing a T_H17 cell population in the adult range and others generating very few cells even by 1 year of age (Fig. 1C). These data, along with published literature demonstrating stimulation of T_H17 cell development by intestinal microbes (15), suggested the possibility that different infant gut microbiotas stimulated these different developmental trajectories.

Infant diet (breast-feeding versus bottle-feeding) influences the intestinal microbiome

To determine if different T_H17 cell development could be related to different microbial colonization of the intestine, we studied microbial colonization and immune cell development in six infant macaques raised indoors by their mothers [dam-reared and breast-fed (DR)] versus six raised in the nursery [nursery-reared and bottle-fed (NR)].

The microbiotas of stool samples taken at 6 and 12 months were assessed by 16S ribosomal RNA (rRNA) profiling on third-generation PhyloChips. Comparison of gross microbial community metrics showed divergence between the rearing groups as early as 6 months, with a trend to greater richness, evenness, and Shannon index diversity in dam-reared animals (Fig. 2A). Despite the fact that identical diet and housing conditions were established by 1 year of age, the differences in these metrics grew larger and were statistically significant at the later time point (Fig. 2A; $P = 0.04$). Furthermore, principal component (PC) analysis of taxon abundance data clearly separated the two rearing groups at both 6 and 12 months of age (Fig. 2B). Permutational multivariate analysis of variance indicated a significant relationship between rearing conditions and divergent microbiota at both time points (adonis; $P = 0.002$ and $P = 0.024$ at 6 and 12 months, respectively).

At the level of abundance of individual taxa, rearing groups showed significant differences at both time points (that is, 6 months, 68 taxa; 12 months, 484 taxa having q value <0.05, with those of largest change shown in Fig. 2C and table S1; see Materials and Methods). By 12 months of age, DR animals had microbiota enriched in members of *Prevotella and Ruminococcus* (Fig. 2, C and D). NR animals had microbiota enriched in members of *Clostridium*. Many of these differences had been established by 6 months of age and grew more extreme over time between rearing groups, suggesting a lasting impact of initial microbial colonization on the juvenile gut microbiota (Fig. 2D). For example, *Prevotella and Lactobacillus* increased in relative abundance over time in the DR group, whereas these genera decreased over the same period in the NR group (Fig. 2D, top left and bottom right panels). In contrast, *Clostridium* representation decreased in both DR and NR animals over the period examined, remaining significantly higher in the NR group ($P = 0.008$ and $P = 0.002$ at 6 and 12 months by Wilcoxon rank sum test).

Breast-fed but not bottle-fed macaque infants develop robust T_H17 cell populations

To examine the possible effects of different gut microbiota composition on immune cell development, we isolated peripheral blood mononuclear cells (PBMCs) from each study animal at 5, 6, 9, and 12 months of age. Extensive immunophenotyping was then performed using a set of four flow cytometry panels defining more than 115 phe-notypes of interest, including antigen-presenting cell and T cell surface, activation, and homing markers. These data were then used for unsupervised clustering of the samples just as with bacterial abundance data, above (Fig. 2B). When this process was performed using all cell populations at 5 and 6 months after birth, the algorithm identified clusters that were unrelated to feeding regimen (Fig. 3, A and B). Nevertheless, lasso regression (30) identified a set of incipient differences that did separate the feeding groups at these early ages, most prominently including T_H17 cells as a percentage of all $CD4^+$ T cells or of memory $CD4^+$ T cells.

Breast-fed and bottle-fed macaque immune systems were radically different by 12 months of age, being clearly separated into groups by the Partitioning Around Medoids (PAM) algorithm (Fig. 3D with adonis $P = 0.002$). Immune profiles were also significantly different at 9 months (Fig. 3C with adonis $P = 0.004$). At 12 months, the groups were entirely separate when plotted along the axes of greatest variation (principal components, Fig. 3D) or when clustered by hierarchal clustering (Fig. 3E), indicating that immune cell differences associated with rearing method dominated all the variability detected in peripheral blood. Differences between breast-fed and bottle-fed infants were concentrated in T_H17 cells and markers of immune cell activation (Fig. 3E), with less prominent differences in T_{reg} phenotypes. Among breast-fed infants, T_H17 cells were overrepresented both among all $CD4^+$ T cells and among memory cells, indicating a true T_H17 polarization (Fig. 3, E and F). The percentage of $CD4^+$ T cells expressing interferon (IFN) and IL-17 upon stimulation was increased an average of 15-fold in breast-fed infants as compared to bottle-fed infants (Fig. 3F).

Dam-reared and nursery-reared macaque infants differ at the single-metabolite level

We searched for possible metabolic connections between altered gut microbiota and immune cell development using gas chromatography–mass spectrometry (GC-MS) analysis of chemicals in stool and plasma. Combined stool and plasma metabolite profiles differed between the two rearing groups at both 6 and 12 months, despite convergence in diet by the latter time point (adonis: $P = 0.05$ and $P = 0.04$ at 6 and 12 months, respectively; Fig. 4, A and B). NR animals showed increased amino acids such as asparagine in stool, a finding that is concordant with the results of previous studies (25) (Fig. 4B). Plasma samples also showed differences between rearing groups, principally in lipid metabolites such as oleic, linoleic, icosenoic, and palmitoleic acids and short-chain fatty acid metabolites such as 2- and 3-hydroxybutanoic acid, which all increased in DR animals (Fig. 4B).

We also investigated possible connections between specific metabolites and immune cell subsets using longitudinal regression analysis. Despite the small sample size available, linear mixed-effect regression models associated some plasma concentrations of short-chain fatty acids with T_{reg} cell subsets [Fig. 4C; see (14)]. Specifically, 2-hydroxybutanoic acid was associated with $CD4^+CD25^+127^{low}$ T_{reg} among memory T cells ($P = 0.0098$ for the longitudinal model; 12-month data shown in Fig. 4C). 2-Hydroxyvaleric acid also was associated with T_{reg} among memory T cells ($P = 0.0115$), and 3-hydroxybutanoic acid was associated with both T_{reg} among memory T cells ($P = 0.0012$) and $CD3^+CD4^+CD25^+FOXP3^+$ T cells ($P = 0.021$).

We then focused on metabolites associated with T_H17 cell subsets. We found that arachidonic acid concentrations were positively associated with T_H17 cell subsets in linear mixed effect models using 6- and 12-month data ($P = 1.3 \times 10^{-7}$ and $P = 0.001$ for association with T_H17 cells in all CD4 or in memory CD4 cells, respectively; 12-month data shown in Fig. 5, A and B). We then used regression to investigate possible association of specific bacterial genera with stool arachidonic acid. Association with *Prevotella* spp. was significant ($P = 0.03$; Fig. 5C), and bacteria of this genus have previously been shown to release arachidonic acid in vitro (31). Indeed, we found a network of significant correlations between stool concentrations of arachidonic acid, T_H17 cells, and bacterial genera such as *Prevotella* and *Campylobacter*, concordant with regression results (Fig. 5D).

The association between *Campylobacter* and arachidonic acid concentrations in stool was suggestive but not significant ($P = 0.088$; fig. S1A); previous literature has demonstrated arachidonic acid release by *Campylobacter* (32). The amount of *Campylobacter* at 6 and 12 months was correlated with T_H17 cells and at 12 months with memory T_H17 cells ($P = 0.004$ and $P = 0.005$, respectively; fig. S1, B and C). Both *Pre-votella* and *Campylobacter* were significantly more abundant in DR than in NR animals at 12 months ($P = 0.0008$ and $P = 0.007$, respectively).

Finally, we assessed plasma kynurenine/tryptophan (kyn/trp) ratios to determine if they might account for T_H17 cell abundances in healthy infants because they appear to do so in HIV-infected humans (16). Kyn/trp ratios did not differ significantly by rearing group (fig. S2A). Furthermore, kyn/trp ratios were not associated with various T_H17 cell subsets in longitudinal regression models. We also assessed the relationship between bacteria that

express enzymes in the tryptophan ca-tabolism pathway and T_H17 cell development, using methods similar to those of Vujkovic-Cvijin and colleagues (16). With UniProt, bacterial genera were categorized according to the number of enzymes involved in tryptophan catabolism that they expressed. Individual eOTUs (empirical operational taxonomic units; see Materials and Methods) were then correlated with kyn/trp ratios, and genera were assigned correlation coefficients on the basis of the highest correlated eOTUs within the genus. Here, among healthy infant macaques, we found no significant relationship between the mean correlation rank and number of pathway enzymes expressed (fig. S2B).

Discussion

We demonstrate that infant diet has profound and durable effects on the gut mi-crobiota of macaques, development of their immune system, and metabolite profiles in plasma and stool. These effects may prove important in understanding variable immune responses to vaccination and infection as well as different propensities for the development of autoimmune disease. Furthermore, the longitudinal data we collected proved useful for hypothesis generation about the mechanisms underlying microbiota-driven immune modulation (for example, the relationship between arachidonic acid and T_H17 cells), which may allow for design of interventional experiments and eventually for pharmacologic manipulation of the developing immune system.

Differences between gut microbiotas were pronounced, both in community-level indices and individual taxa, and remained pronounced 6 months after all animals in the study began receiving an identical diet. NR (bottle-fed) animals had decreased community richness, evenness, and diversity. Previous studies have suggested a connection between decreased richness and inflammation, insulin resistance, and overall adiposity (33, 34).

Surprisingly, immune system profiles remained significantly different between rearing groups at 12 months of age, especially in various T_H17 cell subsets. These included both the percentage of T_H17 cells among $CD4^+$ T cells and among memory cells, indicating a true change in immune cell polarization, rather than a global increase in memory cell production. Our finding that differences were most pronounced in these subsets is perhaps not surprising because T_H17 cells are generated as a result of microbial interactions occurring in the gut mucosa and the cells traffic to that tissue (35, 36). DR animals additionally demonstrated increases in $CD4^+$ and $CD8^+$ T cells making IFN-γ (that is, T_H1 cells and cytotoxic T lymphocytes). Indeed, DR animals demonstrated a profile of immune cell activation and proliferation that is consistent generally with a greater ongoing stimulation by bacteria. This difference in immune systems based on diet is congruent with differences in proinflammatory cytokine production documented by O'Sullivan *et al.* (25).

Our study of rhesus macaques uncovered some associations also seen in studies of human infants. Formula-fed human infants demonstrated greater abundance of Clostridia (24) and increased numbers of $CD4^+$ naïve cells (37). Breast-fed human infants also had higher serum concentrations of the anti-inflammatory cytokine transforming growth factor–β2, which we did not test in our rhesus cohort (38).

Metabolomics of plasma and stool revealed differences at the single-metabolite level between rearing groups that were suggestive when compared to previous literature. At both 6 and 12 months, stool levels of amino acid metabolites were generally higher in NR animals, a finding that is congruent with another study of differently reared rhesus macaques (25). Previous studies have demonstrated that short-chain fatty acids regulate T_{reg} induction and homeostasis, at least in mice (12, 14, 39). Indeed, we observed that derivatives of short-chain fatty acids in plasma were associated with T_{reg} frequencies (12, 14, 39). Whereas previous studies have associated higher concentrations of T_H17 cells with reduced tryptophan catabolism, specifically by the kynurenine pathway (16), we found no significant evidence of this effect in our study of uninfected animals.

Longitudinal sampling and comprehensive analysis of samples (microbiome composition by PhyloChip, immunophenotyping by flow cytometry, and metabolomics by GC-MS) allowed us to form testable hypotheses about the mechanisms of microbiota-driven immune modulation via mixed-effects regression. For example, we observed a longitudinal correlation between arachidonic acid and induction of T_H17 cells. Arachidonic acid is present in rhesus macaque breast milk; however, weaning of macaques typically occurs by about 6 months of age, indicating that differences in arachidonic acid concentrations at later time points were not caused by differences in ingestion of the chemical. We therefore ascribe differences in arachidonic acid concentrations to the metabolic activities of the gut microbiota or to host metabolic activities stimulated by the microbiota. Release of arachidonic acid from phospholipid membranes is controlled by phospholipase A_2 (PLA_2) (40). Numerous mammalian cell types and many commensal bacteria express PLA_2, which is regulated by phosphorylation or Ca^{2+}-induced translocation from the cytosol to the cell membrane (41). Previous studies have shown that many bacteria (often Gram-negative) express forms of PLA_2 that can release arachidonic acid (42, 43). Furthermore, bacteria such as *Prevotella* are known to activate cytosolic $PLA_{2\alpha}$ in macro-phages (31, 44). Higher concentrations of some eicosanoids have previously been associated with T_H17 cell expansion (45, 46). For example, prostaglandin E_2 stimulates the production of T_H17-inducing cytokines in cultured macrophages (47), whereas phospholipase blockade in mice led to decreased circulating IL-17 (48). T_H17 cell expansion caused by elevated arachidonic acid could be beneficial for future responses to pathogenic challenge. For example, studies have shown that infants receiving greater amounts of arachidonic acid were less likely to contract HIV from their HIV^+ mothers (49), and higher numbers of T_H17 cells have been associated with lower acute and plateau SIV viral loads (22).

Overall, our findings show that profound differences in macaque infant gut microbiotas are associated with equally profound differences in the immune system and that this association may be mediated by differing metabolomic environments. The immune differences observed were sufficient to completely separate DR and NR animals on the basis of certain parameters, most notably those relevant to activation and differentiation of T cell subsets. Such differences could explain wide variations among humans in vaccine responsiveness or the tendency to develop immune-mediated diseases (50).

Materials and Methods

Study design

Preliminary data indicated that six animals were required in each group to detect a 20% difference in key immunologic parameters with 80% power and an a of 0.05. No animals were excluded from analysis. This was an observational study designed to search for possible differences in the stool microbiota, stool metabolomics, and/or immune systems of breast-fed and bottle-fed rhesus macaques. Twelve rhesus macaque infants were used for the longitudinal study of immune cell phenotypes, microbiota, and metabolomics. Six study animals were raised indoors by their mothers; six were raised indoors in the CNPRC nursery; both infant groups were studied at the same period. All infants were delivered vaginally. Antibiotics were considered to be a confounding variable (51, 52). Medical histories were carefully examined before inclusion to ensure that no animal had been antibiotic-treated or had experienced any apparent enteric illness or abnormality. The study was not blinded.

Ethics statement

The UC Davis animal care program is accredited by the Association for the Assessment and Accreditation of Laboratory Animal Care, International (AAALAC). All animal procedures were approved prior to implementation by the UC Davis Institutional Animal Care and Use Committee and were consistent with the requirements of the Animal Welfare Act. Activities related to animal care were performed as per standard operating procedures at the California National Primate Research Center.

Diet

Dam-reared animals had a diet consisting primarily of breast milk and high-protein monkey chow (LabDiet; present in the cage for dam's diet and normally sampled by infant 1 to 4 weeks after birth) and were in contact with their mothers until the age of about 6 months. The gross compositions of human and rhesus macaque breast milk are similar (53, 54). Both contain numerous components not found in formula, including certain small molecules (53), biological polymers (55–57), microbes (53), and viable whole maternal cells (58); however, rhesus macaque breast milk lacks certain oligosaccharides found in human milk (59). Nursery-reared infants were fed formula (Enfamil Lipil + Iron) and had no contact with their mothers. They received high-protein chow as a supplement to the formula. The diets in both groups converged over time to high-protein chow at the age of 6 months. All animals received seasonal fruits as part of the CNPRC feeding enrichment program during the study; time of fruit introduction and frequency of provision were approximately equal for both groups because all animals were born in the same period.

Sample collection

Stool and blood samples were taken from each rhesus macaque infant at 5, 6, 9, and 12 months after birth. Fresh stool samples were collected from the cage pan in the morning and immediately frozen at −70°C for later DNA extraction for PhyloChip analysis. Plasma samples were stored at −70°C. PBMCs were isolated by gradient density purification using

Lymphocyte Separation Medium (MP Biomedicals, LLC), then washed and cryopreserved in liquid nitrogen.

Stool sample processing and microbiota analysis with PhyloChip

PhyloChip analyses were performed using samples taken at 6 and 12 months only. Fecal specimens were stored at −70°C until processing. Total DNA was isolated using the QIAamp DNA Stool Mini Kit (Qiagen) with slight modifications. Briefly, fecal samples were resuspended in Qiagen's ASL buffer and transferred into Lysing Matrix E tubes (MP Biomedicals). Samples were homogenized in a FastPrep-24 instrument (MP Biomedicals) at 6.0 m/s for 30 s. Beads were pelleted, and the supernatant was transferred into sterile 2-ml microcentrifuge tubes. ASL buffer was added to each LME tube, followed by homogenization at 6 m/s for 30 s. Beads were pelleted, and the supernatant was combined with the supernatant from the first extraction step. DNA isolation was completed as outlined in the QIAamp DNA Stool Mini Kit manual. DNA was eluted in 150 μl of distilled water and stored at −20°C All samples yielded sufficient total DNA for downstream processing. The bacterial 16S rRNA genes were amplified in almost full length in a temperature gradient using the primers 27F (5′-AGAGTTTGATCCTGGCTCAG-3′) (60) and 1492R (5′-GGTTACCTTGTTACGACTT-3′) (60, 61).

Polymerase chain reactions (PCRs) for PhyloChip analysis were performed in 25-μl reactions containing 0.02 U/μL of Ex Taq (Takara Mirus Bio Inc.), 1× Takara buffer with $MgCl_2$, 27F and 1492R primers (0.3 pmol/μl) (60), 0.8 mM deoxynucleotide triphosphates, bovine serum albumin (0.8 mg/ml) (Roche Applied Science), and 30 ng of DNA template. A total of 12 reactions per sample were performed in an Eppendorf Mastercycler gradient thermocycler across a gradient (48° to 58.4°C) of annealing temperatures to maximize diversity recovered. Reaction conditions were as follows: initial denaturation (95°C for 3 min) followed by 25 cycles of 95°C (30 s), annealing (30 s), and extension at 72°C (2 min) and a final extension of 72°C (10 min). PCR reactions were pooled and purified using the QIAquick PCR Purification Kit (Qiagen). Amplification was verified by 1% tris-borate EDTA agarose gel electrophoresis. Two hundred fifty nanograms of amplicon per sample plus quantitative standards (consisting of 14 non-16S rRNA genes that permit data normalization) were fragmented, biotinylated, and applied to each PhyloChip Array, version G3. PhyloChip arrays were washed, stained, and scanned using a GeneArray scanner (Affymetrix) (61, 62). A pixel image was captured for each scan, and intensities were determined using standard Affymetrix software (GeneChip Mcroarray Analysis Suite). Hybridization values and the fluorescence intensity (proportional to RNA levels) for each taxon were determined by using a trimmed average. To calculate the eOTUs, probe sets (groups of probes) were determined empirically on the basis of both (i) taxonomic relatedness of the probes and (ii) their correlation in fluorescence intensity throughout the experiment. The empirical probe set was taxonomically annotated with a Bayesian method directly from the oligomers within the probes.

Immune cell phenotyping by flow cytometry

Flow cytometric analysis—Frozen rhesus macaque PBMCs were thawed and stained for flow cytometry. Predetermined optimal concentrations of the following antibodies were

used: anti-CD3-Alexa 700 (clone SP34-2), anti-CD3-Pacific Blue (PacBlue) (clone SP34-2), anti-CD95-APC (allophycocyanin) (clone DX2), anti-CD95-FITC (fluorescein isothiocyanate) (clone DX2), anti-CD28-APC-H7 (clone CD28.2), anti-CCR5–APC (clone 3A9), anti-Ki67–Alexa 488 (clone B56), anti–IFN-γ–phycoerythrin (PE)-Cy7 (clone B27), anti-CD127–PE (clone HIL-7R-M21), anti-CD25–PE-Cy7 (clone M-A251), anti-CD196–PE (clone 11A9), anti-CD194–Alexa 647 (clone 1G1), anti-CD123–peridinin chlorophyll protein–Cy5.5 (clone 7G3), anti–HLA (human leukocyte antigen)-DR–PE-Cy7 (clone 646.6), anti-CD16– PacBlue (clone 3G8), anti-CD83–PE (clone HB15e), anti-CD80–FITC (clone L307.4), anti-CD86–APC (clone 2331 FUN-1) (all from BD); anti-CD8–PE-Cy5.5 (clone 3B5), anti-CD14–Qdot 605 (clone TUK4), anti– CD20–electron-coupled dye (ECD) (clone HI47), Aqua Live/Dead amine dye–AmCyan (Invitrogen); IL-17–PE (clone eBio64CAP17), anti-CD11c– Alexa 700 (clone 3.9) (eBioscience); anti-FOXP3–PacBlue (clone 206D), anti-CD28–Alexa 700 (clone CD28.2) (BioLegend); anti-CD4–Qdot 655 (19Thy5D7), anti-CD38–PE (clone OKT10) (NHP reagents); and anti– HLA ECD (clone Immu-357) (Beckman Coulter). A minimum of 300,000 events were collected for each sample. Compensation controls were prepared with antibody capture beads (BD Biosciences) stained separately with individual monoclonal antibodies. Analysis was performed using FlowJo version X (10.0.6 release).

Intracellular cytokine staining—Levels of cytokine-producing cells were determined by cytokine flow cytometry after in vitro stimulation with phorbol 12-myristate 13-acetate (PMA) and ionomycin. Rhesus macaque PBMCs were resuspended to 10^6 cells/ml in complete RPMI 1640 medium. Cells were then incubated for 6 hours at 37°C in medium containing PMA (50 ng/ml) (Sigma-Aldrich), ionomycin (1 μg/ml) (Sigma-Aldrich), and GolgiPlug (5 μg/ml) (BD Biosciences). After incubation, cells were washed and stained with surface markers. Cells were then washed, permeabilized using a Cytofix/Cytoperm kit (BD Biosciences) according to the manufacturer's instructions, intracellularly stained, washed, fixed in phosphate-buffered saline containing 1% paraformaldehyde, and acquired on an LSR II cytometer.

Metabolomic analysis

Plasma and stool were analyzed for the presence and relative quantity of metabolites using GC–time-of-flight MS at 6 and 12 months (West Coast Metabolomics Center at UC Davis). Additionally, concentrations of kynurenine and tryptophan were quantified by liquid chromatography–tandem MS, as previously described (63). Morning plasma cortisol levels (samples collected between 8:30 and 9:30 AM) were tested by enzyme-linked immunosorbent assay and were not higher among nursery-reared and formula-fed infants.

Statistical analysis

Statistical analysis was performed in the R programming environment. Unless otherwise noted, all plots were created using ggplot2.

Microbial populations—Community indices, including richness, evenness, and Shannon diversity, were calculated using the Vegan package in R. The function adonis was used to assess correlations between dissimilarity of samples and factors such as rearing within the

same software package. Principal component analysis was performed using the ade4 package. A two-tailed unpaired *t* test was used to identify bacteria eOTUs found to be significantly different between rearing groups. These significance values were then adjusted for false discovery using the *q* value package. The *q* value of a test measures the proportion of false positives incurred (called the false discovery rate) when that particular test is called significant. In the case of dam-reared animals, the 50 statistically significant eOTUs with the highest Δ (increased in DR with Δ >3.5 $\log_2$ fluorescence intensity) were included (Fig. 2C), and the 38 statistically significant eOTUs with the highest Δ (increased in NR with Δ >0.94) were included (Fig. 2C). Fewer NR-increased eOTUs were included because only 38 eOTUs met both *P* and *q* value criteria for significance.

Immune cell subsets—The same procedures were followed for statistical analysis of immune cell data for all time points. Wilcoxon rank sum tests were used to identify immune cell subsets found to be significantly different between the two rearing groups. To create the heat map, those immune cell subsets that were found significantly different between rearing groups were rescaled using the scales package. For each immune cell subset, values were rescaled from percentage units to a range from 0 to 1. These new values were then plotted into a heat map. To assess progression of immunophenotypic profile, we used the ade4 package to perform principal component analysis based on data from 12-month samples. Using loadings from this time point, we then applied these loadings to immune data from 5, 6, and 9 months. After centering the data using a custom script, we plotted the data on uniform axes.

Metabolomics data—Each metabolite was subjected to a two-tailed unpaired *t* test, assuming unequal variance and correcting for false discovery using the *q* value package (done on total metabolites - stool and plasma samples). Those found significantly different between rearing groups ($P < 0.05$) were grouped by type of metabolism [based on assignments in KEGG (Kyoto Encyclopedia of Genes and Genomes) Pathway for each metabolite] and displayed in waterfall plots.

Analysis of plasma kyn/trp ratios—Spearman correlation coefficients (*R* values) for each eOTU abundance were calculated in relation to plasma kyn/trp. For fig. S2B, each genus was ranked on the basis of *R* values for the eOTUs in that genus with the highest *R* value. These genera were then ranked by *R* value and divided by the number of enzymes in the kynurenine pathway for tryptophan catabolism that each genus was inferred to express. Inferences were made by browsing the UniProt Consortium database (64) (http://www.uniprot.org) by taxonomy for each of the enzymes in the pathway (Enzyme Commission nos. EC 1.13.11.11, EC 3.5.1.9, EC 3.7.1.3, and EC 1.14.13.9).

Data analysis—To assess possible relations between microbial genera, immune cell subsets, and metabolites, we performed hierarchical clustering on a combined data set of all variables. To evaluate possible relationships between microbial genera, immune cell subsets, and metabolites, we performed linear mixed-effects regression using the lmer command in the lme4 package. Significance of random effects was assessed on the basis of likelihood ratio test between nested models.

Supplementary Material

Refer to Web version on PubMed Central for supplementary material.

Acknowledgments

We thank J. Lee and P.-M. Sosa for assistance with sample collection; S. Iwai, K. E. Fujimura, and J. Mar for assistance with PhyloChip experiments and analysis; I. Vujkovic-Cvijin and J. M. McCune for their assistance in interpretation of kynurenine-tryptophan results; the West Coast Metabolomics Center at UC Davis, directed by O. Fiehn, for expert services; and A. Tarantal for editorial suggestions.

Funding: Research reported in this publication was supported by the National Institute of Allergy and Infectious Diseases, NIH under award no. K23AI081540 to D.J.H.-O., by the Bill and Melinda Gates Foundation under a "Grand Challenges Exploration" award (#52094) to D.J.H.-O., and by the Office of the Director of NIH under grant P51-OD011107 to the CNPRC.

References and Notes

1. Lozupone CA, Stombaugh JI, Gordon JI, Jansson JK, Knight R. Diversity, stability and resilience of the human gut microbiota. Nature. 2012; 489:220–230. [PubMed: 22972295]
2. McKenna P, Hoffmann C, Minkah N, Aye PP, Lackner A, Liu Z, Lozupone CA, Hamady M, Knight R, Bushman FD. The macaque gut microbiome in health, lentiviral infection, and chronic enterocolitis. PLOS Pathog. 2008; 4:e20. [PubMed: 18248093]
3. Pantoja-Feliciano IG, Clemente JC, Costello EK, Perez ME, Blaser MJ, Knight R, Dominguez-Bello MG. Biphasic assembly of the murine intestinal microbiota during early development. ISME J. 2013; 7:1112–1115. [PubMed: 23535917]
4. Guarner F, Malagelada JR. Gut flora in health and disease. Lancet. 2003; 361:512–519. [PubMed: 12583961]
5. Hsiao EY, McBride SW, Hsien S, Sharon G, Hyde ER, McCue T, Codelli JA, Chow J, Reisman SE, Petrosino JF, Patterson PH, Mazmanian SK. Microbiota modulate behavioral and physiological abnormalities associated with neurodevelopmental disorders. Cell. 2013; 155:1451–1463. [PubMed: 24315484]
6. Khosravi A, Mazmanian SK. Breathe easy: Microbes protect from allergies. Nat Med. 2012; 18:492–494. [PubMed: 22481405]
7. Schwartz S, Friedberg I, Ivanov IV, Davidson LA, Goldsby JS, Dahl DB, Herman D, Wang M, Donovan SM, Chapkin RS. A metagenomic study of diet-dependent interaction between gut microbiota and host in infants reveals differences in immune response. Genome Biol. 2012; 13:r32. [PubMed: 22546241]
8. Seekatz AM, Panda A, Rasko DA, Toapanta FR, Eloe-Fadrosh EA, Khan AQ, Liu Z, Shipley ST, Detolla LJ, Sztein MB, Fraser CM. Differential response of the cynomolgus macaque gut microbiota to Shigella infection. PLOS One. 2013; 8:e64212. [PubMed: 23755118]
9. Weng M, Walker WA. The role of gut microbiota in programming the immune phenotype. J Dev Orig Health Dis. 2013; 4:203–214. [PubMed: 24353893]
10. Wingender G, Stepniak D, Krebs P, Lin L, McBride S, Wei B, Braun J, Mazmanian SK, Kronenberg M. Intestinal microbes affect phenotypes and functions of invariant natural killer T cells in mice. Gastroenterology. 2012; 143:418–428. [PubMed: 22522092]
11. Round JL, Mazmanian SK. Inducible Foxp3^{+} regulatory T-cell development by a commensal bacterium of the intestinal microbiota. Proc Natl Acad Sci U S A. 2010; 107:12204–12209. [PubMed: 20566854]
12. Atarashi K, Tanoue T, Oshima K, Suda W, Nagano Y, Nishikawa H, Fukuda S, Saito T, Narushima S, Hase K, Kim S, Fritz JV, Wilmes P, Ueha S, Matsushima K, Ohno H, Olle B, Sakaguchi S, Taniguchi T, Morita H, Hattori M, Honda K. T_{reg} induction by a rationally selected mixture of Clostridia strains from the human microbiota. Nature. 2013; 500:232–236. [PubMed: 23842501]

13. Atarashi K, Tanoue T, Shima T, Imaoka A, Kuwahara T, Momose Y, Cheng G, Yamasaki S, Saito T, Ohba Y, Taniguchi T, Takeda K, Hori S, Ivanov II, Umesaki Y, Itoh K, Honda K. Induction of colonic regulatory T cells by indigenous Clostridium species. Science. 2011; 331:337–341. [PubMed: 21205640]

14. Smith PM, Howitt MR, Panikov N, Michaud M, Gallini CA, Bohlooly-Y M, Glickman JN, Garrett WS. The microbial metabolites, short-chain fatty acids, regulate colonic T_{reg} cell homeostasis. Science. 2013; 341:569–573. [PubMed: 23828891]

15. Ivanov II, Atarashi K, Manel N, Brodie EL, Shima T, Karaoz U, Wei D, Goldfarb KC, Santee CA, Lynch SV, Tanoue T, Imaoka A, Itoh K, Takeda K, Umesaki Y, Honda K, Littman DR. Induction of intestinal Th17 cells by segmented filamentous bacteria. Cell. 2009; 139:485–498. [PubMed: 19836068]

16. Vujkovic-Cvijin I, Dunham RM, Iwai S, Maher MC, Albright RG, Broadhurst MJ, Hernandez RD, Lederman MM, Huang Y, Somsouk M, Deeks SG, Hunt PW, Lynch SV, McCune JM. Dysbiosis of the gut microbiota is associated with HIV disease progression and tryptophan catabolism. Sci Transl Med. 2013; 5:193ra191.

17. Zelante T, Iannitti RG, Cunha C, De Luca A, Giovannini G, Pieraccini G, Zecchi R, D'Angelo C, Massi-Benedetti C, Fallarino F, Carvalho A, Puccetti P, Romani L. Tryptophan catabolites from microbiota engage aryl hydrocarbon receptor and balance mucosal reactivity via interleukin-22. Immunity. 2013; 39:372–385. [PubMed: 23973224]

18. Blankson JN. Control of HIV-1 replication in elite suppressors. Discov Med. 2010; 9:261–266. [PubMed: 20350494]

19. Petrovski S, Fellay J, Shianna KV, Carpenetti N, Kumwenda J, Kamanga G, Kamwendo DD, Letvin NL, McMichael AJ, Haynes BF, Cohen MS, Goldstein DB. Center for HIV/AIDS Vaccine Immunology, Common human genetic variants and HIV-1 susceptibility: A genome-wide survey in a homogeneous African population. AIDS. 2011; 25:513–518. [PubMed: 21160409]

20. Pereyra F, Jia X, McLaren PJ, Telenti A, de Bakker PI, Walker BD, Ripke S, Brumme CJ, Pulit SL, Carrington M, Kadie CM, Carlson JM, Heckerman D, Graham RR, Plenge RM, Deeks SG, Gianniny L, Crawford G, Sullivan J, Gonzalez E, Davies L, Camargo A, Moore JM, Beattie N, Gupta S, Crenshaw A, Burtt NP, Guiducci C, Gupta N, Gao X, Qi Y, Yuki Y, Piechocka-Trocha A, Cutrell E, Rosenberg R, Moss KL, Lemay P, O'Leary J, Schaefer T, Verma P, Toth I, Block B, Baker B, Rothchild A, Lian J, Proudfoot J, Alvino DM, Vine S, Addo MM, Allen TM, Altfeld M, Henn MR, Le Gall S, Streeck H, Haas DW, Kuritzkes DR, Robbins GK, Shafer RW, Gulick RM, Shikuma CM, Haubrich R, Riddler S, Sax PE, Daar ES, Ribaudo HJ, Agan B, Agarwal S, Ahern RL, Allen BL, Altidor S, Altschuler EL, Ambardar S, Anastos K, Anderson B, Anderson V, Andrady U, Antoniskis D, Bangsberg D, Barbaro D, Barrie W, Bartczak J, Barton S, Basden P, Basgoz N, Bazner S, Bellos NC, Benson AM, Berger J, Bernard NF, Bernard AM, Birch C, Bodner SJ, Bolan RK, Boudreaux ET, Bradley M, Braun JF, Brndjar JE, Brown SJ, Brown K, Brown ST, Burack J, Bush LM, Cafaro V, Campbell O, Campbell J, Carlson RH, Carmichael JK, Casey KK, Cavacuiti C, Celestin G, Chambers ST, Chez N, Chirch LM, Cimoch PJ, Cohen D, Cohn LE, Conway B, Cooper DA, Cornelson B, Cox DT, Cristofano MV, Cuchural G Jr, Czartoski JL, Dahman JM, Daly JS, Davis BT, Davis K, Davod SM, DeJesus E, Dietz CA, Dunham E, Dunn ME, Ellerin TB, Eron JJ, Fangman JJ, Farel CE, Ferlazzo H, Fidler S, Fleenor-Ford A, Frankel R, Freedberg KA, French NK, Fuchs JD, Fuller JD, Gaberman J, Gallant JE, Gandhi RT, Garcia E, Garmon D, Gathe JC Jr, Gaultier CR, Gebre W, Gilman FD, Gilson I, Goepfert PA, Gottlieb MS, Goulston C, Groger RK, Gurley TD, Haber S, Hardwicke R, Hardy WD, Harrigan PR, Hawkins TN, Heath S, Hecht FM, Henry WK, Hladek M, Hoffman RP, Horton JM, Hsu RK, Huhn GD, Hunt P, Hupert MJ, Illeman ML, Jaeger H, Jellinger RM, John M, Johnson JA, Johnson KL, Johnson H, Johnson K, Joly J, Jordan WC, Kauffman CA, Khanlou H, Killian RK, Kim AY, Kim DD, Kinder CA, Kirchner JT, Kogelman L, Kojic EM, Korthuis PT, Kurisu W, Kwon DS, LaMar M, Lampiris H, Lanzafame M, Lederman MM, Lee DM, Lee JM, Lee MJ, Lee ET, Lemoine J, Levy JA, Llibre JM, Liguori MA, Little SJ, Liu AY, Lopez AJ, Loutfy MR, Loy D, Mohammed DY, Man A, Mansour MK, Marconi VC, Markowitz M, Marques R, Martin JN, Martin HL Jr, Mayer KH, McElrath MJ, McGhee TA, McGovern BH, McGowan K, McIntyre D, Mcleod GX, Menezes P, Mesa G, Metroka CE, Meyer-Olson D, Miller AO, Montgomery K, Mounzer KC, Nagami EH, Nagin I, Nahass RG, Nelson MO, Nielsen C, Norene DL, O'Connor DH, Ojikutu BO, Okulicz J, Oladehin OO, Oldfield EC III, Olender SA, Ostrowski

M, Owen WF Jr, Pae E, Parsonnet J, Pavlatos AM, Perlmutter AM, Pierce MN, Pincus JM, Pisani L, Price LJ, Proia L, Prokesch RC, Pujet HC, Ramgopal M, Rathod A, Rausch M, Ravishankar J, Rhame FS, Richards CS, Richman DD, Rodes B, Rodriguez M, Rose RC III, Rosenberg ES, Rosenthal D, Ross PE, Rubin DS, Rumbaugh E, Saenz L, Salvaggio MR, Sanchez WC, Sanjana VM, Santiago S, Schmidt W, Schuitemaker H, Sestak PM, Shalit P, Shay W, Shirvani VN, Silebi VI, Sizemore JM Jr, Skolnik PR, Sokol-Anderson M, Sosman JM, Stabile P, Stapleton JT, Starrett S, Stein F, Stellbrink HJ, Sterman FL, Stone VE, Stone DR, Tambussi G, Taplitz RA, Tedaldi EM, Telenti A, Theisen W, Torres R, Tosiello L, Tremblay C, Tribble MA, Trinh PD, Tsao A, Ueda P, Vaccaro A, Valadas E, Vanig TJ, Vecino I, Vega VM, Veikley W, Wade BH, Walworth C, Wanidworanun C, Ward DJ, Warner DA, Weber RD, Webster D, Weis S, Wheeler DA, White DJ, Wilkins E, Winston A, Wlodaver CG, van't Wout A, Wright DP, Yang OO, Yurdin DL, Zabukovic BW, Zachary KC, Zeeman B, Zhao M. International HIV Controllers Study. The major genetic determinants of HIV-1 control affect HLA class I peptide presentation. Science. 2010; 330:1551–1557. [PubMed: 21051598]

21. Favre D, Lederer S, Kanwar B, Ma ZM, Proll S, Kasakow Z, Mold J, Swainson L, Barbour JD, Baskin CR, Palermo R, Pandrea I, Miller CJ, Katze MG, McCune JM. Critical loss of the balance between Th17 and T regulatory cell populations in pathogenic SIV infection. PLOS Pathog. 2009; 5:e1000295. [PubMed: 19214220]
22. Hartigan-O'Connor DJ, Abel K, Van Rompay KK, Kanwar B, McCune JM. SIV replication in the infected rhesus macaque is limited by the size of the preexisting T_H17 cell compartment. Sci Transl Med. 2012; 4:136ra169.
23. McGeachy MJ, McSorley SJ. Microbial-induced Th17: Superhero or supervillain? J Immunol. 2012; 189:3285–3291. [PubMed: 22997231]
24. Hascoët JM, Hubert C, Rochat F, Legagneur H, Gaga S, Emady-Azar S, Steenhout PG. Effect of formula composition on the development of infant gut microbiota. J Pediatr Gastroenterol Nutr. 2011; 52:756–762. [PubMed: 21593648]
25. O'Sullivan A, He X, McNiven EM, Haggarty NW, Lönnerdal B, Slupsky CM. Early diet impacts infant rhesus gut microbiome, immunity, and metabolism. J Proteome Res. 2013; 12:2833–2845. [PubMed: 23651394]
26. Walker WA. Initial intestinal colonization in the human infant and immune homeostasis. Ann Nutr Metab. 2013; 63(Suppl. 2):8–15. [PubMed: 24217032]
27. Zetterström R, Bennet R, Nord KE. Early infant feeding and micro-ecology of the gut. Acta Paediatr Jpn. 1994; 36:562–571. [PubMed: 7825464]
28. Elmore DB, Anderson JH, Hird DW, Sanders KD, Lerche NW. Diarrhea rates and risk factors for developing chronic diarrhea in infant and juvenile rhesus monkeys. Lab Anim Sci. 1992; 42:356–359. [PubMed: 1434494]
29. Hartigan-O'Connor DJ, Abel K, McCune JM. Suppression of SIV-specific $CD4^+$ T cells by infant but not adult macaque regulatory T cells: Implications for SIV disease progression. J Exp Med. 2007; 204:2679–2692. [PubMed: 17954571]
30. Tibshirani R. Regression shrinkage and selection via the lasso. J R Statist Soc B (Methodol). 1996; 58:267–288.
31. Hiller G, Sternby M, Sundler R, Wijkander J. Phosphatidylinositol 3-kinase in zymosan- and bacteria-induced signalling to mobilisation of arachidonic acid in macrophages. Biochim Biophys Acta. 2000; 1485:163–172. [PubMed: 10832097]
32. Istivan TS, Coloe PJ, Fry BN, Ward P, Smith SC. Characterization of a haemolytic phospholipase A_2 activity in clinical isolates of *Campylobacter concisus*. J Med Microbiol. 2004; 53:483–493. [PubMed: 15150326]
33. Cotillard A, Kennedy SP, Kong LC, Prifti E, Pons N, Le Chatelier E, Almeida M, Quinquis B, Levenez F, Galleron N, Gougis S, Rizkalla S, Batto JM, Renault P, ANR MicroObes consortium. Doré J, Zucker JD, Clément K, Ehrlich SD. Dietary intervention impact on gut microbial gene richness. Nature. 2013; 500:585–588. [PubMed: 23985875]
34. Le Chatelier E, Nielsen T, Qin J, Prifti E, Hildebrand F, Falony G, Almeida M, Arumugam M, Batto JM, Kennedy S, Leonard P, Li J, Burgdorf K, Grarup N, Jørgensen T, Brandslund I, Nielsen HB, Juncker AS, Bertalan M, Levenez F, Pons N, Rasmussen S, Sunagawa S, Tap J, Tims S, Zoetendal G, Brunak S, Clément K, Doré J, Kleerebezem M, Kristiansen K, Renault P, Sicheritz-

Ponten T, de Vos WM, Zucker JD, Raes J, Hansen T, MetaHIT consortium. Bork P, Wang J, Ehrlich SD, Pedersen O. Richness of human gut microbiome correlates with metabolic markers. Nature. 2013; 500:541–546. [PubMed: 23985870]

35. Cook DN, Prosser DM, Forster R, Zhang J, Kuklin NA, Abbondanzo SJ, Niu XD, Chen SC, Manfra DJ, Wiekowski MT, Sullivan LM, Smith SR, Greenberg HB, Narula SK, Lipp M, Lira SA. CCR6 mediates dendritic cell localization, lymphocyte homeostasis, and immune responses in mucosal tissue. Immunity. 2000; 12:495–503. [PubMed: 10843382]
36. Singh SP, Zhang HH, Foley JF, Hedrick MN, Farber JM. Human T cells that are able to produce IL-17 express the chemokine receptor. J Immunol. 2008; 180:214–221. [PubMed: 18097022]
37. Andersson Y, Hammarström ML, Lönnerdal B, Graverholt G, Fält H, Hernell O. Formula feeding skews immune cell composition toward adaptive immunity compared to breastfeeding. J Immunol. 2009; 183:4322–4328. [PubMed: 19734215]
38. Kainonen E, Rautava S, Isolauri E. Immunological programming by breast milk creates an anti-inflammatory cytokine milieu in breast-fed infants compared to formula-fed infants. Br J Nutr. 2013; 109:1962–1970. [PubMed: 23110822]
39. Furusawa Y, Obata Y, Fukuda S, Endo TA, Nakato G, Takahashi D, Nakanishi Y, Uetake C, Kato K, Kato T, Takahashi M, Fukuda NN, Murakami S, Miyauchi E, Hino S, Atarashi K, Onawa S, Fujimura Y, Lockett T, Clarke JM, Topping DL, Tomita M, Hori S, Ohara O, Morita T, Koseki H, Kikuchi J, Honda K, Hase K, Ohno H. Commensal microbe-derived butyrate induces the differentiation of colonic regulatory T cells. Nature. 2013; 504:446–450. [PubMed: 24226770]
40. Leslie CC. Regulation of the specific release of arachidonic acid by cytosolic phospholipase A_2. Prostaglandins Leukot Essent Fatty Acids. 2004; 70:373–376. [PubMed: 15041029]
41. Rodríguez M, Domingo E, Municio C, Alvarez Y, Hugo E, Fernández N, Sánchez Crespo M. Polarization of the innate immune response by prostaglandin E_2: A puzzle of receptors and signals. Mol Pharmacol. 2014; 85:187–197. [PubMed: 24170779]
42. Istivan TS, Coloe PJ. Phospholipase A in Gram-negative bacteria and its role in pathogenesis. Microbiology. 2006; 152:1263–1274. [PubMed: 16622044]
43. Bejar R, Curbelo V, Davis C, Gluck L. Premature labor. II. Bacterial sources of phospholipase. Obstet Gynecol. 1981; 57:479–482. [PubMed: 7017516]
44. Svensson U, Houweling M, Holst E, Sundler R. Phosphorylation and activation of the arachidonate-mobilizing phospholipase A_2 in macrophages in response to bacteria. Eur J Biochem. 1993; 213:81–86. [PubMed: 8386632]
45. Chizzolini C, Chicheportiche R, Alvarez M, de Rham C, Roux-Lombard P, Ferrari-Lacraz S, Dayer JM. Prostaglandin E_2 synergistically with interleukin-23 favors human Th17 expansion. Blood. 2008; 112:3696–3703. [PubMed: 18698005]
46. Yao C, Sakata D, Esaki Y, Li Y, Matsuoka T, Kuroiwa K, Sugimoto Y, Narumiya S. Prostaglandin E_2–EP4 signaling promotes immune inflammation through T_H1 cell differentiation and T_H17 cell expansion. Nat Med. 2009; 15:633–640. [PubMed: 19465928]
47. Gagliardi MC, Teloni R, Mariotti S, Bromuro C, Chiani P, Romagnoli G, Giannoni F, Torosantucci A, Nisini R. Endogenous PGE2 promotes the induction of human Th17 responses by fungal β-glucan. J Leukoc Biol. 2010; 88:947–954. [PubMed: 20807707]
48. Marusic S, Thakker P, Pelker JW, Stedman NL, Lee KL, McKew JC, Han L, Xu X, Wolf SF, Borey AJ, Cui J, Shen MW, Donahue F, Hassan-Zahraee M, Leach MW, Shimizu T, Clark JD. Blockade of cytosolic phospholipase A_2a prevents experimental autoimmune encephalomyelitis and diminishes development of Th1 and Th17 responses. J Neuroimmunol. 2008; 204:29–37. [PubMed: 18829119]
49. Villamor E, Koulinska IN, Furtado J, Baylin A, Aboud S, Manji K, Campos H, Fawzi WW. Long-chain n–6 polyunsaturated fatty acids in breast milk decrease the risk of HIV transmission through breastfeeding. Am J Clin Nutr. 2007; 86:682–689. [PubMed: 17823433]
50. Hansen SG, Ford JC, Lewis MS, Ventura AB, Hughes CM, Coyne-Johnson L, Whizin N, Oswald K, Shoemaker R, Swanson T, Legasse AW, Chiuchiolo MJ, Parks CL, Axthelm MK, Nelson JA, Jarvis MA, Piatak M Jr, Lifson JD, Picker LJ. Profound early control of highly pathogenic SIV by an effector memory T-cell vaccine. Nature. 2011; 473:523–527. [PubMed: 21562493]

51. Ferrer M, Martins dos Santos VA, Ott SJ, Moya A. Gut microbiota disturbance during antibiotic therapy: A multi-omic approach. Gut Microbes. 2013; 5:64–70. [PubMed: 24418972]
52. Rooks MG, Veiga P, Wardwell-Scott LH, Tickle T, Segata N, Michaud M, Gallini CA, Beal C, van Hylckama-Vlieg JE, Ballal SA, Morgan XC, Glickman JN, Gevers D, Huttenhower C, Garrett WS. Gut microbiome composition and function in experimental colitis during active disease and treatment-induced remission. ISME J. 2014; 8:1403–1417. [PubMed: 24500617]
53. O'Sullivan A, He X, McNiven EM, Hinde K, Haggarty NW, Lönnerdal B, Slupsky CM. Metabolomic phenotyping validates the infant rhesus monkey as a model of human infant metabolism. J Pediatr Gastroenterol Nutr. 2013; 56:355–363. [PubMed: 23201704]
54. Hinde K, Milligan LA. Primate milk: Proximate mechanisms and ultimate perspectives. Evol Anthropol. 2011; 20:9–23. [PubMed: 22034080]
55. Anderson NG, Powers MT, Tollaksen SL. Proteins of human milk. I. Identification of major components. Clin Chem. 1982; 28:1045–1055. [PubMed: 6804119]
56. Joseph CL, Havstad S, Bobbitt K, Woodcroft K, Zoratti EM, Nageotte C, Misiak R, Enberg R, Nicholas C, Ezell JM, Ownby DR, Johnson CC. Transforming growth factor beta ($TGF\beta_1$) in breast milk and indicators of infant atopy in a birth cohort. Pediatr Allergy Immunol. 2014; 25:257–263. [PubMed: 24520941]
57. Rogier EW, Frantz AL, Bruno ME, Wedlund L, Cohen DA, Stromberg AJ, Kaetzel CS. Secretory antibodies in breast milk promote long-term intestinal homeostasis by regulating the gut microbiota and host gene expression. Proc Natl Acad Sci USA. 2014; 111:3074–3079. [PubMed: 24569806]
58. Field CJ. The immunological components of human milk and their effect on immune development in infants. J Nutr. 2005; 135:1–4. [PubMed: 15623823]
59. Goto K, Fukuda K, Senda A, Saito T, Kimura K, Glander KE, Hinde K, Dittus W, Milligan LA, Power ML, Oftedal OT, Urashima T. Chemical characterization of oligosaccharides in the milk of six species of New and Old World monkeys. Glycoconj J. 2010; 27:703–715. [PubMed: 21127965]
60. Lane, DJ. Nucleic Acid Techniques in Bacterial Systematics. Stackebrandt, E.; Goodfellow, M., editors. Wiley; New York, NY: 1991. p. 115-148.
61. DeSantis TZ, Brodie EL, Moberg JP, Zubieta IX, Piceno YM, Andersen GL. High-density universal 16S rRNA microarray analysis reveals broader diversity than typical clone library when sampling the environment. Microb Ecol. 2007; 53:371–383. [PubMed: 17334858]
62. Masuda N, Church GM. *Escherichia coli* gene expression responsive to levels of the response regulator EvgA. J Bacteriol. 2002; 184:6225–6234. [PubMed: 12399493]
63. Favre D, Mold J, Hunt PW, Kanwar B, Loke P, Seu L, Barbour JD, Lowe MM, Jayawardene A, Aweeka F, Huang Y, Douek DC, Brenchley JM, Martin JN, Hecht FM, Deeks SG, McCune JM. Tryptophan catabolism by indoleamine 2,3-dioxygenase 1 alters the balance of T_H17 to regulatory T cells in HIV disease. Sci Transl Med. 2010; 2:32ra36.
64. UniProt Consortium. Reorganizing the protein space at the Universal Protein Resource (UniProt). Nucleic Acids Res. 2012; 40:D71–D75. [PubMed: 22102590]

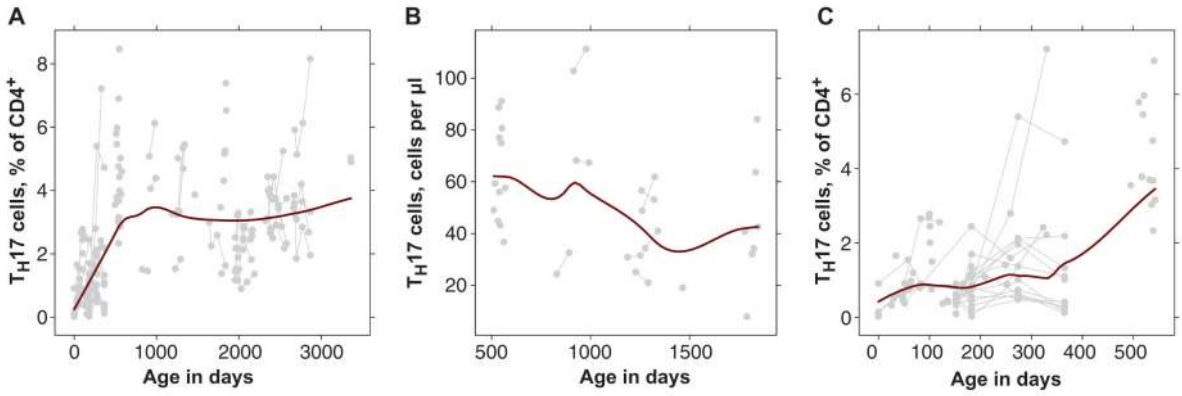

Fig. 1. Circulating T_H17 cells throughout the macaque life span

(**A**) Percentage of T_H17 cells among $CD4^+$ T cells in peripheral blood, from birth to more than 9 years of age. Data points are connected by lines wherever they represent longitudinal samples from one animal. The curve shown is a loess curve plotted in R using a span value of 0.6. **(B)** Absolute numbers of circulating T_H17 cells in rhesus macaques aged 17 to 62 months. The slight decrease seen is not significant in mixed-effects regression ($P = 0.06$). (C) Development of T_H17 cells throughout the first 18 months of life. As in (A), the percentage of T_H17 cells among $CD4^+$ T cells in peripheral blood is shown. The curve shown is a loess curve; the increase shown is highly significant in mixed-effects regression ($P < 0.00005$).

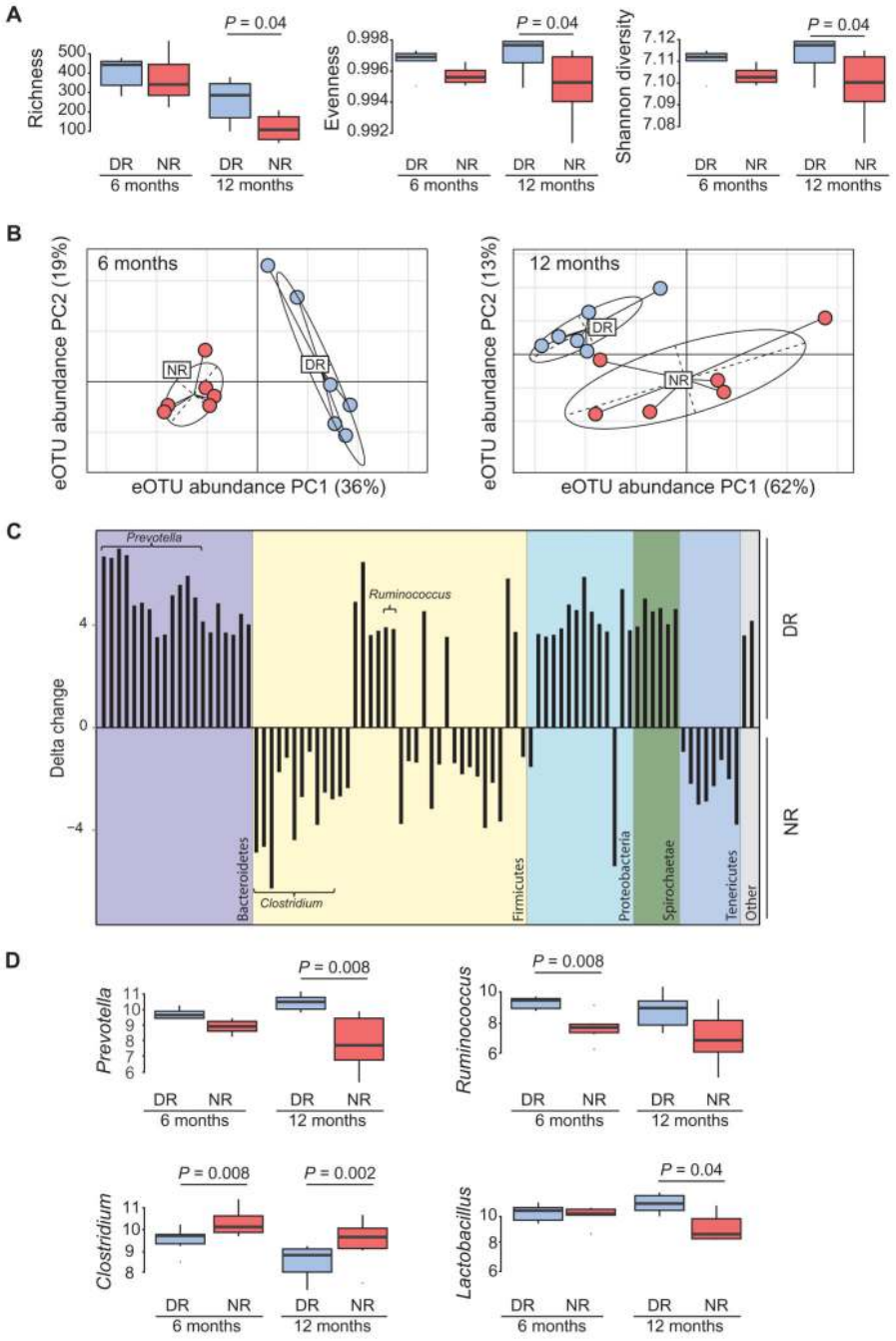

Fig. 2. Different gut microbiotas in dam-reared and nursery-reared animals at 6 and 12 months of age

(**A**) Richness, evenness, and Shannon index diversity are higher in dam-reared (DR) compared with nursery-reared (NR) animals. **(B)** Principal component analysis shows clear separation of NR and DR gut microbiotas at 6 and 12 months. Note that interindividual distances in these plots are generally reflective of Bray-Curtis dissimilarities. **(C)** Waterfall plot showing Δ abundance of taxa that are statistically different between rearing groups. Δ abundance is calculated by subtraction of average abundance in one rearing group from

average abundance in another. **(D)** Abundance of genera based on pooled data from taxa assigned to each.

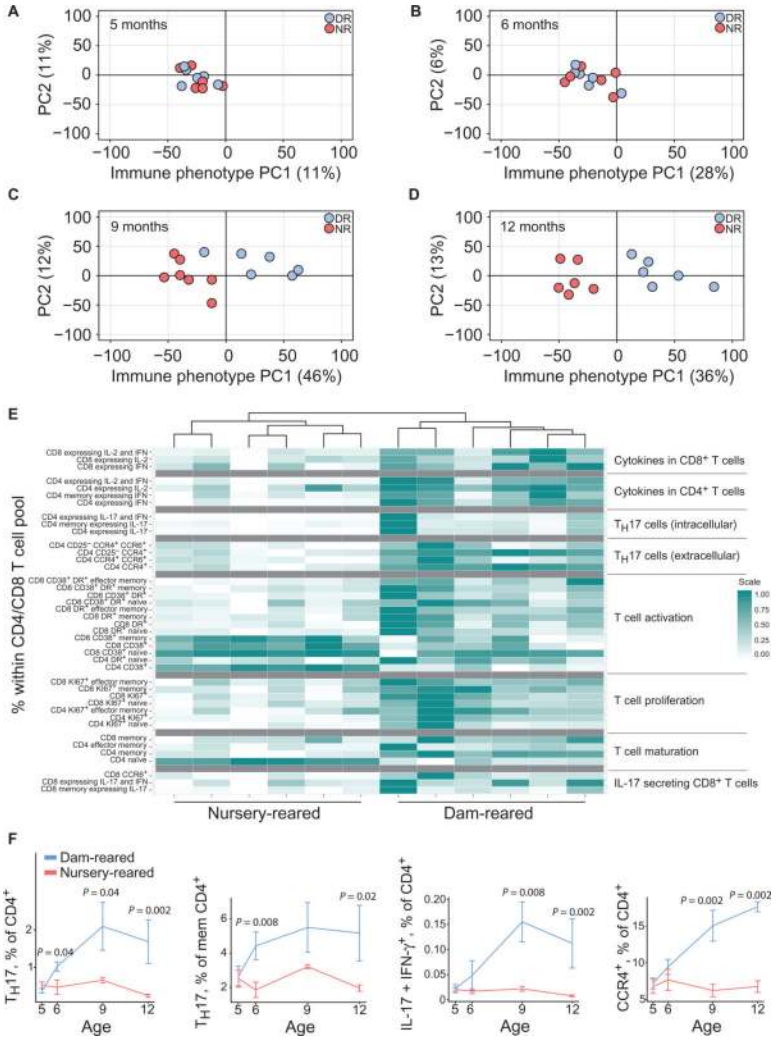

Fig. 3. Dam-reared animals harbor robust T_H17 cell populations

(**A** to **D)** Principal component analysis of immune cell abundances at (A) 5, (B) 6, (C) 9, and (D) 12 months, all plotted using loadings from the 12-month immune cell profile. **(E)** Heat map showing scaled values for various T cell subsets that were found to be statistically different between rearing groups. Animals (shown as columns) were clustered using hclust. **(F)** Populations of various immune cell subsets over time. Lines represent averages for rearing groups with SE brackets.

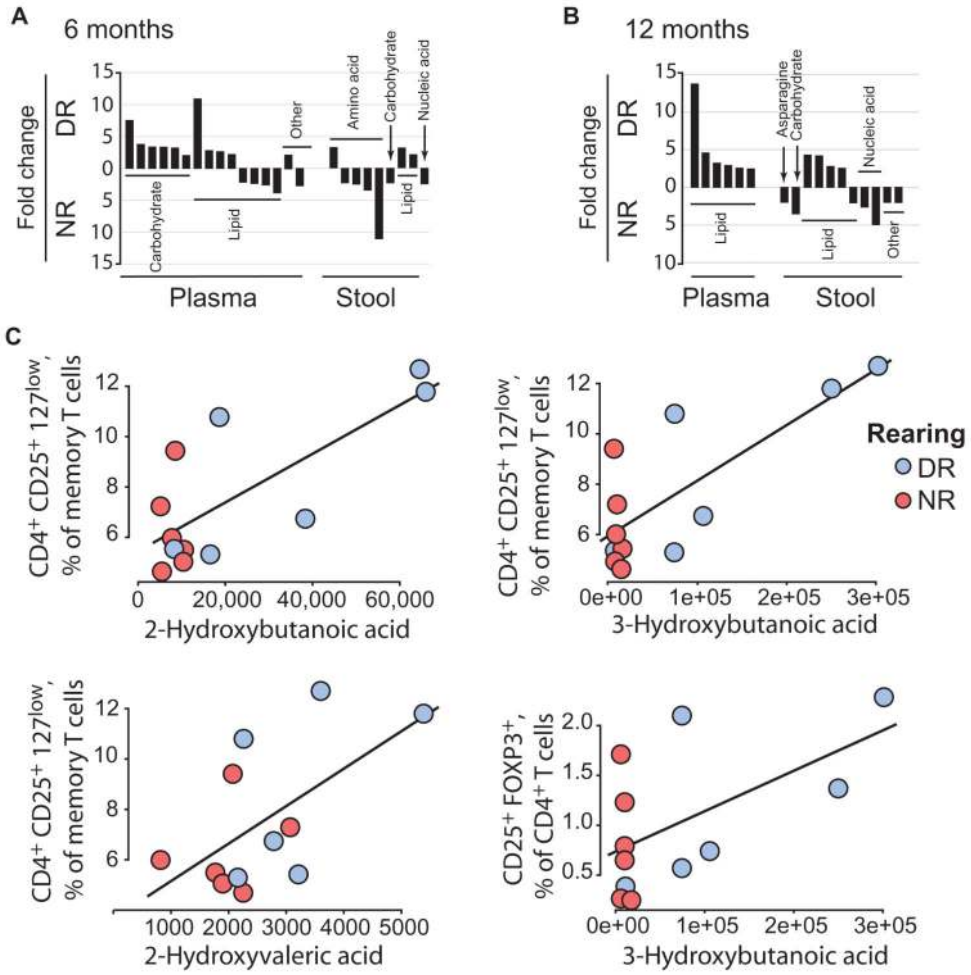

Fig. 4. Metabolomic profiles differ between rearing groups

(**A** to **B**) Waterfall plots of statistically significantly different metabolites at (A) 6 and (B) 12 months, defined by $P < 0.05$ and fold change > 2. **(C)** Scatterplots with regression lines for T_{reg} populations and short-chain fatty acids found in plasma at 12 months. All metabolites are plotted using absorbance units.

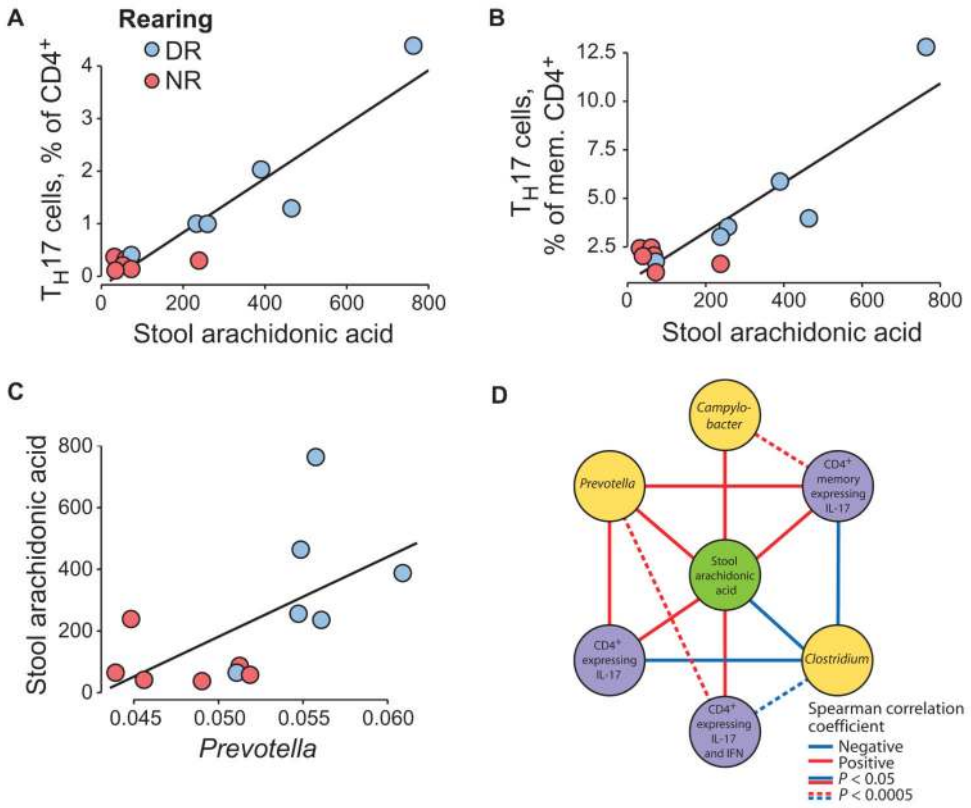

Fig. 5. Relationship between arachidonic acid concentrations and T_H17 cell abundance

(**A** to **B**) Scatterplot and longitudinal regression show a significant association between stool arachidonic acid and (A) T_H17 cells or (B) memory T_H17 cells. **(C)** Significant association between arachidonic acid concentrations and *Prevotella*. All panels show 12-month data. **(D)** Significant correlations between stool concentrations of arachidonic acid, T_H17 cells, and bacterial genera plotted in network form.